LA-6949-MS, Revised

c. 3

Los Alamos National Laboratory is operated by the University of California for the United States Department of Energy under contract W-7405-ENG-36.

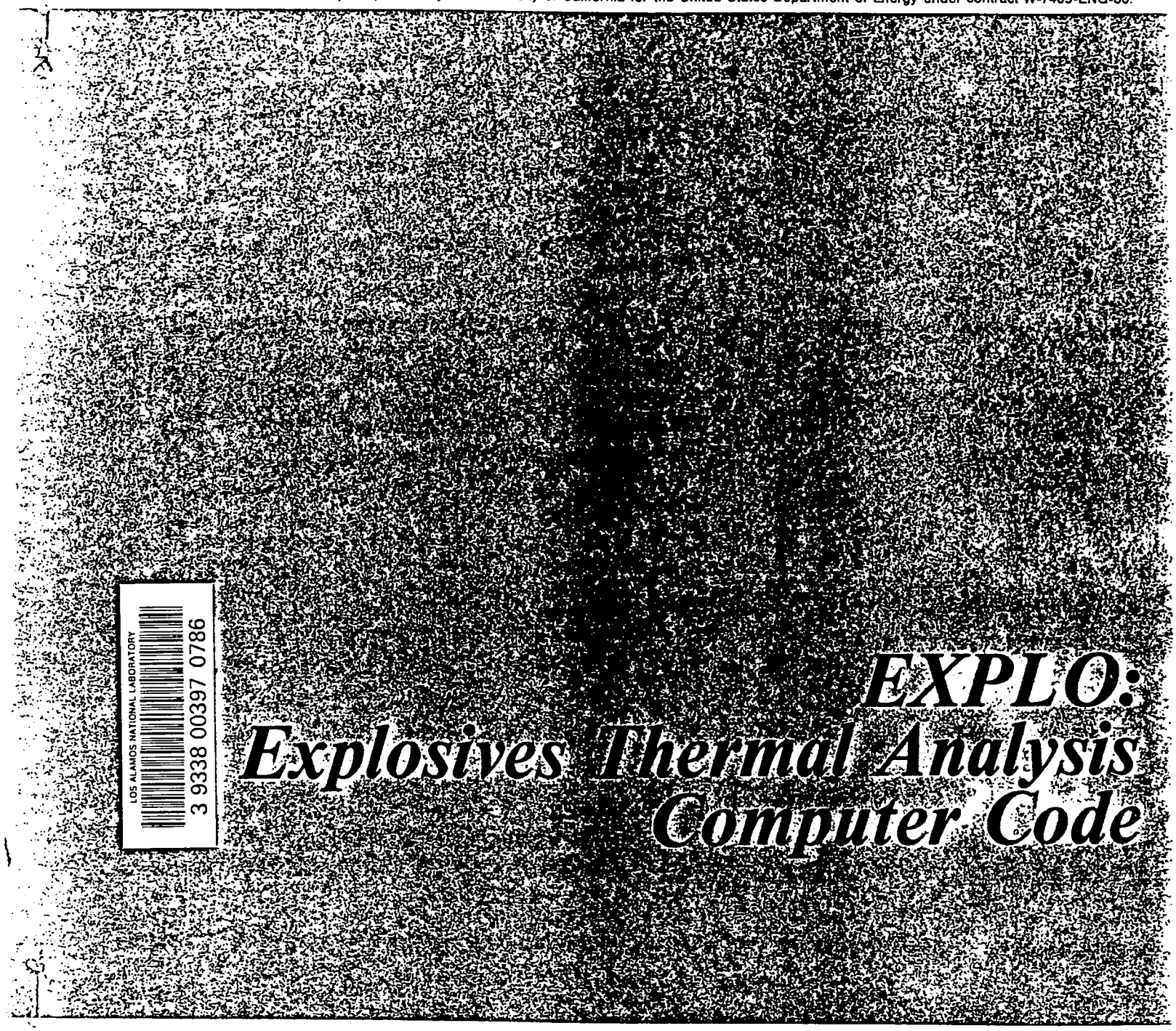

EXPLO: Explosives Thermal Analysis Computer Code

Los Alamos
Los Alamos National Laboratory
Los Alamos, New Mexico 87545

This report was issued originally in January 1978.

LA-6949-MS, Revised

UC-45
Issued: September 1981

EXPLO: Explosives Thermal Analysis Computer Code

Dwight L. Jaeger

Los Alamos National Laboratory
Los Alamos, New Mexico 87545

CONTENTS

EXPLO: EXPLOSIVES THERMAL ANALYSIS COMPUTER CODE

by

Dwight L. Jaeger

ABSTRACT

The finite difference method is used to calculate temperature fields and times to initiation for explosive materials. The code is one-dimensional and is programmed for Cartesian, cylindrical, and spherical coordinates. Temperature-dependent properties, phase changes, and multiple heat source terms are allowed. Multiple source terms use Nth-order Arrhenius kinetics for each material component. Temperature, flux, convection, or radiation boundary conditions may be employed. Internal convection is considered for materials that undergo a solid-liquid phase change. The Crank-Nicholson implicit solution method, which allows large time steps and short running time, is used.

I. INTRODUCTION

WX Division of the Los Alamos National Laboratory has been concerned with thermal initiation of explosives for many years. Stringent weapons safety requirements, aerodynamic heating in low-altitude high-speed aircraft, and explosives that are in contact with radioactive materials are examples of the thermal initiation problems of current interest. The code EXPLO is a derivative of the TEPLO code developed by Anderson.[1] EXPLO deviates from TEPLO in the following major areas: (1) variable conductivity between each node, (2) Nth-order rather than zero-order Arrhenius kinetics, (3) multiple heat generation terms, and (4) internal convection for melt problems.

EXPLO solves the conduction equation with N source terms:[2]

$$\rho C_p \frac{\partial T}{\partial \tau} = \nabla(k\nabla T) + \sum_{j=1}^{N} \rho\left(S_j - W_j\right)^N Q_j Z_j e^{-E_j/RT} + QJ + \rho QI \qquad (1)$$

$$+ \rho F Q_m (T - T_f) \quad ,$$

where W must obey

$$\frac{dW_j}{dT} = (S_j - W_j)^N e^{-E/RT} \qquad (2)$$

and where

T = temperature,
τ = time,
ρ = density,
C_p = heat capacity,
k = thermal conductivity,
S = original fraction of species j,
W = current burned fraction of species j,
N = reaction order,
Q = heat of reaction,
Z = collision number,
E/R= activation temperature,
QJ = heat input at layer interfaces,
QI = heat generation,
T_f = transition (melt) temperature,
F = constant, and
Q_m = phase transition energy.

For problems involving melt and internal convection a free convection analysis is performed, which uses Prandtl and Grashof numbers to determine the Nusselt number. This is then used to determine an effective thermal boundary layer

thickness. Finally, the thermal conductivity of the liquid region outside the thermal boundary layer is increased artificially to simulate the heat flow caused by the free movement of the liquid region. The conduction equation [Eq. (1)] can then be used to simulate the conduction-convection problem.

II. THERMAL ANALYSIS THEORY

A. Problem Description

EXPLO was developed as a heat transfer tool for a variety of explosives thermal initiation problems. These include aerodynamic heating of external weapons on high-speed aircraft, irradiated materials in contact with explosives, the possibility of exposure of weapons to fire, and many others. The high explosives can have nonlinear material properties, internal heat generation, and phase changes, which most heat transfer codes can not handle. A one-dimensional, multilayer, finite difference approach was selected for this computer code. Temperature, flux, and convective external boundary conditions were required. The capability for either temperature or energy initialization was required with an exponential form for the energy initialization. Phase change and internal convection were required for materials, such as TNT, that melt long before ignition temperatures are reached. Nth-order Arrhenius kinetics with multiple species were also required to simulate mixed explosives. The code uses either steady-state or transient boundary conditions, with either fixed or variable time steps. The classical convection analysis using Prandtl, Reynolds, Grashof, and Nusselt numbers is incorporated into the code.

B. External Convection Analysis

Routines are available within EXPLO to perform either free or forced convection on the external boundary. The free convection analysis assumes a vertical plate theory and uses the correlation[3]

$$N_{NU} = C(N_{GR}N_{PR})^{m}$$

with the following coefficients and exponents.

$N_{GR}N_{PR}$	C	m
$0 < N_{GR}N_{PR} < 2713$	1.585	0.125
$2713 < N_{GR}N_{PR} < 8.378 \times 10^7$	0.59	0.25
$8.378 \times 10^7 < N_{GR}N_{PR} < \infty$	0.129	0.33333

The exact location of the transition between coefficients and exponents, based on the product of Grashof and Prandtl numbers, was selected to give a piecewise smooth correlation with the Nusselt number. The analysis is reasonably accurate for vertical plates and vertical cylinders. EXPLO uses this analysis for all problems, including spherical problems, and thus caution is in order.

The forced convection analysis uses three continuous correlations among the Nusselt, Prandtl, and Reynolds numbers from a flat plate theory.[3]

$$0 < N_{RE} < 3305$$

$$N_{NU} = 0.332\, N_{PR}^{1/3}\, N_{RE}^{1/2} \qquad (3)$$

$$3305 < N_{RE} < 2{,}846{,}758$$

$$N_{NU} = 0.0292\, N_{PR}^{1/3}\, N_{RE}^{0.8}$$

$$2{,}846{,}758 < N_{RE}$$

$$N_{NU} = .185\, N_{PR}^{1/3}\, \frac{N_{RE}}{(\log N_{RE})^{2.584}}$$

The flat plate theory was used to develop the programmed correlations, and further code development may be required for certain cylindrical and spherical problems.

C. Internal Convection Analysis

TNT thermal initiation experiments conducted at Los Alamos[4] indicated that a substantial amount of internal convection was taking place in the liquid TNT. To simulate the convection phenomena, a model was devised that calculated the effective thermal boundary layers and then artificially increased the

conductivity of the material that was above the melting point and outside the boundary layer. In this way a conduction code can simulate the heat conduction plus the heat transport. To illustrate this point, consider a vertical heated plate (Fig. 1). The low-density hot air near the wall tends to rise, establishing a velocity profile and a thermal boundary layer. The classical definition of a boundary layer is

$$\frac{T_w - T_{BL}}{T_w - T_{AMB}} = 0.99 \quad , \tag{4}$$

where

T_w = wall temperature,
T_{BL} = temperature at maximum thickness, and
T_{AMB} = ambient temperature.

Therefore, there is sufficient mixing in the fluid outside the boundary layer to maintain a temperature gradient near zero. The internal convection problem can be simulated by defining an effective boundary layer with a resistance to heat flow equal to the real boundary layer's resistance and then setting the conductivity of the free moving fluid sufficiently high to restrain the temperature variations in this region to <1%. The interface resistance can be calculated by using the free convection correlations, defined in Sec. II. B., to define the Nusselt number, and hence h, the convection coefficient. Then, using the relation for equal thermal resistance, it follows that

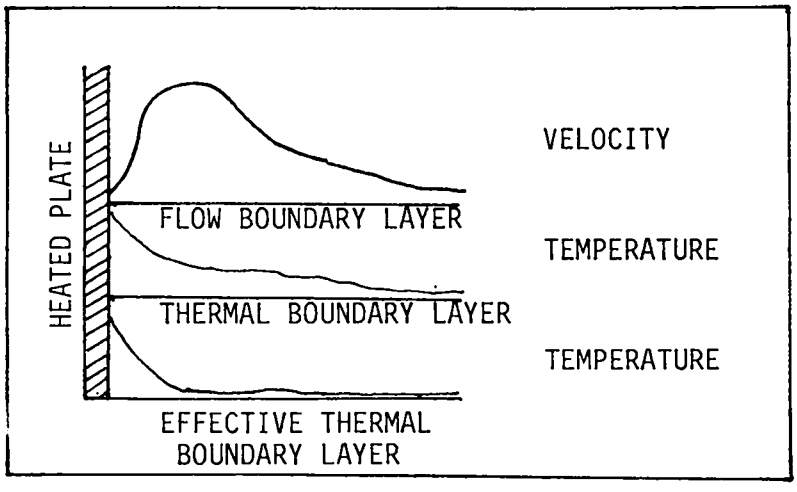

Fig. 1.
Vertical heated plate.

$$\frac{q}{A} = h(T_w - T_{AMB}) = \frac{k\Delta T}{\Delta X} \quad , \tag{5}$$

where

q = heat flow,
A = area,
h = convection coefficient,
T_w = wall temperature,
T_{AMB} = ambient temperature,
k = conductivity,
ΔT = temperature drop in boundary layer, and
ΔX = boundary layer thickness.

This can be rewritten to define the effective thermal boundary layer as

$$X_{eff} = \frac{k}{h} \quad . \tag{6}$$

The internal convection problem is thereby reduced to a conduction problem that uses both the real conductivity of the fluid in the boundary layer and the conduction through the central portion of the fluid pool with its conductivity made high enough to ensure a <1% deviation of the temperature through the boundary layer.

D. Conduction Analysis

The previous sections defined the boundary conditions and translated the internal convection problem into a conduction problem. The solution to this conduction problem is different from Anderson's classical solution[1] in that the thermal conductivity variations at the fluid-boundary layer intersection are now large, and the intersection moves with time.

The conduction equation [Eq. (1)] can be expanded, using a Taylor series expansion, and formulated according to the Crank-Nicholson method[5] to give

$$T'_m - \frac{(1-\beta)\Delta\tau}{C_p} FQ_m T'_m - \frac{\alpha\Delta\tau}{\Delta r^2}(1-\beta)\left[T'_{m+1} + T'_{m-1} - 2T'_m + \frac{K\Delta r}{2r}\left(T'_{m+1} - T'_{m-1}\right)\right] \quad (7)$$

$$= T_m + \frac{\beta\Delta\tau}{C_p} FQ_m T_m + \frac{\alpha\Delta\tau}{\Delta r^2}\beta\left[T_{m+1} + T_{m-1} - 2T_m + \frac{K\Delta r}{2r}\left(T_{m+1} - T_{m-1}\right)\right]$$

$$+ \frac{\Delta\tau}{C_p}\sum_{j=1}^{N}\left(S_j - W_{mj}\right) Q_j Z_j e^{-E_j/RT_m} + \frac{\Delta\tau}{\rho C_p}\left(QJ + \rho QI - \rho FQ_m T_f\right) \quad .$$

where

T' = temperature at a new time step;

m = node number;

K = 0, 1, or 2 for Cartesian, cylindrical, or spherical geometry, respectively;

α = thermal diffusity;

τ = time;

r = spacial coordinate;

S = initial species fraction;

W = species at τ;

Q = heat of decomposition;

Z = collision number;

E/R = activation temperature; and

β = 0-backward difference, .5-Crank-Nicholson, 1-forward difference.

Equation (7) can be simplified to give

$$-C_1(1-\beta)T'_{m-1} + \left[CC - \frac{\rho\Delta r^2}{k} FQ_m(1-\beta) + 2(1-\beta)\right] T'_m - C_2(1-\beta)T_{m+1} \quad (8)$$

$$= \beta C_1 T_{m-1} + \left(CC + \frac{\beta\rho\Delta r^2}{k} FQ_m - 2\beta\right) T_m + \beta C_2 T_{m+1}$$

$$+ \frac{\rho\Delta r^2}{k}\sum_{j=1}^{N}\left(S_j - W_{mj}\right) Q_j Z_j e^{-E_j/RT_m} + \frac{\Delta r^2}{k}\left(QJ + \rho QI - \rho FQ_m T_f\right) \quad ,$$

where

$$CC = \frac{\Delta r^2}{\alpha\Delta\tau} \quad ,$$

$$C_1 = 1 - \frac{K\Delta r}{2r} \quad , \text{ and}$$

$$C_2 = 1 + \frac{K\Delta r}{2r} \quad .$$

Equation (8) is valid over a region of equally spaced intervals with constant conductivity. The normal finite difference scheme applies Eq. (8) over a defined layer and adds a dummy node at each end of the layer for the boundary conditions or layer intersections.[1] However, if a melt transition is moving through a layer in which the conductivity of the liquid differs from the solid, the temperature distribution is not calculated correctly. The solution is to consider all layers to be one element thick and to use two dummy nodes to define the interface with the next element. The dummy nodes may then be eliminated algebraically to give a matrix equal in size to that of a one-layer problem and smaller than that in a multilayer problem solved by the conventional procedure.

The nodal pattern (Fig. 2) consists of one real element and two boundary elements for each node. Equation (8) is valid for node m with the boundary conditions in which the temperature and flux must be continuous. Thus, for the boundary between nodes ℓ and m, the boundary conditions are

$$\frac{q}{A} = k_\ell \frac{T_\ell - T_{\ell+1}}{\Delta X_\ell} = k_m \frac{T_{m-1} - T_m}{\Delta X_m} \quad , \tag{9}$$

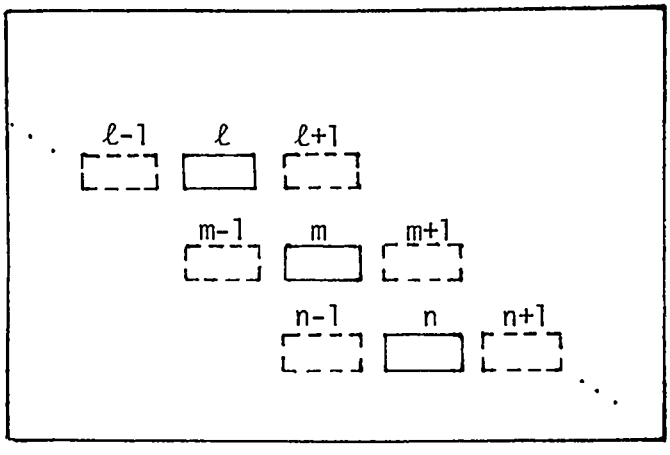

Fig. 2.
Nodal Pattern

and

$$\frac{T_{\ell} + T_{\ell+1}}{2} = \frac{T_{m-1} + T_m}{2} \quad , \tag{10}$$

where

k_{ℓ} = conductivity of element ℓ,
k_m = conductivity of element m,
ΔX_{ℓ} = size of element ℓ, and
ΔX_m = size of element m.

Solving Eq. (10) for $T_{\ell+1}$, substituting the result into Eq. (9), and solving for T_{m-1} gives

$$T_{m-1} = \frac{1 - n_{\ell m}}{1 + n_{\ell m}} T_m + \frac{2n_{\ell m}}{1 + n_{\ell m}} T_{\ell} \quad , \tag{11}$$

where

$$n_{\ell m} = \frac{k_{\ell} \Delta X_m}{k_m \Delta X_{\ell}} \quad .$$

A similar expression can be derived for the interface between m and n giving

$$T_{m+1} = \frac{1 - n_{nm}}{1 + n_{nm}} T_m + \frac{2n_{nm}}{1 + n_{nm}} T_n \quad , \tag{12}$$

where

$$n_{nm} = \frac{k_n \Delta X_m}{k_m \Delta X_n} \quad .$$

Substitution of Eqs. (11) and (12) into Eq. (8) gives the final form of the conduction equation:

$$-(1-\beta)C_1 \frac{2n_{\ell m}}{1+n_{\ell m}} T'_{\ell} + \left[CC - (1-\beta)\frac{\rho\Delta r^2}{K} FQ_m + 2(1-\beta) - C_1(1-\beta)\left(\frac{1-n_{\ell m}}{1+n_{\ell m}}\right)\right. \quad (13)$$

$$\left. - (1-\beta)C_2\left(\frac{1-n_{nm}}{1+n_{nm}}\right)\right] T'_m - (1-\beta)C_2 \frac{2n_{nm}}{1+n_{nm}} T'_n$$

$$= \beta C_1 \frac{2n_{\ell m}}{1+n_{\ell m}} T_{\ell} + \left[CC + \frac{\beta\rho\Delta r^2}{K} FQ_m - 2\beta + \beta C_1\left(\frac{1-n_{\ell m}}{1+n_{\ell m}}\right) + \beta C_2\left(\frac{1-n_{nm}}{1+n_{nm}}\right)\right] T_m$$

$$+ \beta C_2 \frac{2n_{nm}}{1+n_{nm}} T_n + \frac{\rho\Delta r^2}{K} \sum_{j=1}^{N} \left(S_j - W_{m,j}\right) Q_j Z_j e^{-E_j/RT_m}$$

$$+ \frac{\Delta r^2}{K} (QJ + \rho QI) \quad .$$

Equation (13) is an implicit equation capable of large time steps and it can be solved by Gaussian elimination. It is valid for all interior nodes and is unaffected by layer intersections. Note that if $\Delta X_m = \Delta X_n$ and $k_m = k_n$ (on the interior of a given layer), then $n_{nm} = 1$, $n_{\ell m} = 1$, and Eq. (13) reduces to a more conventional equation.[1,3,4]

Temperature, flux, and convection boundary conditions are of interest in thermal initiation problems. If node ℓ (Fig. 2) is on the boundary and a temperature is imposed on the boundary between it and the dummy node ℓ-1, the average temperature of the two nodes must equal the boundary temperature (T_0); thus, the temperature boundary condition can be stated as

$$T_1 + T_2 = 2T_0 \quad . \quad (14)$$

The flux boundary condition is obtained from Fourier's conduction law, which states (defined for heat flow into the system as positive)

$$\frac{q}{A} = k \frac{dT}{dX} \quad . \quad (15)$$

A Taylor series expansion of Eq. (15) provides the final form for the flux boundary condition,

$$T_1 - T_2 = \frac{q\Delta X}{k} \quad . \tag{16}$$

The convection-radiation boundary condition is obtained by equating Newton's law of cooling to Fourier's conduction law:

$$\varepsilon G \left[T_R^4 - \left(\frac{T_1 + T_2}{2} \right)^4 \right] + h \left(T_0 - \frac{T_1 + T_2}{2} \right) = \frac{q}{A} = k \frac{dT}{dX} \quad . \tag{17}$$

A Taylor series expansion of Eq. (17) provides the final form of the convection-radiation boundary condition,

$$\left[1 + \frac{h\Delta X}{2k} + \frac{\varepsilon\sigma\Delta X}{16K} (T_1 + T_2)^3 \right] T_1 + \left[-1 + \frac{h\Delta X}{2k} + \frac{\varepsilon\sigma\Delta X}{16K} (T_1 + T_2)^3 \right] T_2$$
$$= \frac{h\Delta X}{k} T_0 + \frac{\varepsilon\sigma\Delta X}{K} T_R^4 \quad . \tag{18}$$

Equations (14), (16), and (18) are the boundary equations where subscript 0 refers to ambient temperature, subscript 1 refers to the dummy boundary node, subscript 2 refers to the first real node, and subscript R refers to the radiation ambient temperature. The boundary conditions can be combined with the conduction equation [Eq. (13)] to generate a Crank-Nicholson tridiagonal matrix (D_{ij}) of the form

$$\begin{bmatrix}
D_{11} & D_{12} & 0 & 0 & \cdots & & & 0 \\
D_{21} & D_{22} & D_{23} & 0 & \cdots & & & 0 \\
0 & D_{32} & D_{33} & D_{34} & \cdots & & & 0 \\
\vdots & \vdots & \vdots & \vdots & & \vdots & & \vdots \\
0 & 0 & D_{i,i-1} & D_{ii} & D_{i,i+1} & 0 \cdots & & 0 \\
\vdots & \vdots & \vdots & \vdots & \vdots & \vdots & & \vdots \\
0 & \cdots & & 0 & 0 & D_{k-1,k-2} & D_{k-1,k-1} & D_{k-1,k} \\
0 & \cdots & & 0 & 0 & 0 & D_{k,k-1} & D_{kk}
\end{bmatrix}$$

where the conduction equation has the form

$$\left|D_{ij}\right| \left|T_i\right| = \left|V_i\right| , \tag{19}$$

where

$$D_{11} = D_{kk} = 1.0, \text{ or } -1.0, \text{ or } 1.0 + \frac{h\Delta X}{2k} + \frac{\sigma\epsilon\Delta T}{16K} (T_1 + T_2)^3 \tag{20}$$

and

$$D_{12} = D_{k,k-1} = 1.0, \text{ or } -1.0, \text{ or } -1.0 + \frac{h\Delta X}{2k} + \frac{\sigma\epsilon\Delta T}{16K} (T_1 + T_2)^3 \tag{21}$$

for temperature, flux, or convection-radiation boundary conditions, respectively; and where

$$D_{i,i-1} = \frac{2C_1 n_{\ell m}}{1 + n_{\ell m}} (1-\beta) , \tag{22}$$

$$D_{i,i} = CC + \left[2 - C_1 \left(\frac{1 - n_{\ell m}}{1 + n_{\ell m}}\right) - C_2 \left(\frac{1 - n_{nm}}{1 + n_{nm}}\right) - \frac{\rho\Delta r^2 FQ_m}{k}\right] (1-\beta) , \tag{23}$$

$$D_{i,\,i+1} = \frac{2C_2 n_{nm}}{1 + n_{nm}} (1-\beta) , \tag{24}$$

and also

$$V_1 = V_n = 2T_0, \text{ or } \frac{q\Delta X}{k} , \text{ or } \frac{h\Delta XT}{k} + \frac{\sigma\epsilon\Delta X}{k} T_R^4 \tag{25}$$

for temperature, flux, or convection boundary conditions, respectively; and finally, where

$$V_i = \frac{2\beta C_1 n_{\ell m}}{1 + n_{\ell m}} T_{i-1} + \left[CC - 2\beta + \beta C_1 \left(\frac{1 - n_{\ell m}}{1 + n_{\ell m}} \right) + \beta C_2 \left(\frac{1 - n_{nm}}{1 + n_{nm}} \right) \right] T_i \qquad (26)$$

$$+ \frac{\beta \rho \Delta r^2}{K} FQ_m T_i + \frac{2\beta C_2 n_{nm}}{1 + n_{nm}} T_{i+1} + \frac{\rho \Delta r^2}{K} \sum_{j=1}^{N} \left(S_j - W_{i,j} \right) Q_j Z_j e^{-E_j/RT_m}$$

$$+ \frac{\Delta r^2}{K} (QJ + \rho QI) - \frac{\rho \Delta r^2}{K} FQ_m T_m \quad .$$

The above analysis has been programmed for the CDC 7600 and VAX/VMS computers at Los Alamos and is used to simulate a variety of tests. Temperature distribution errors and energy check errors were prevalent in all problems before the $n_{\ell m}$ and n_{nm} were included in the analysis. There was an early attempt to fix the error problems by including the nonlinear term $\delta k \delta T / \delta X \delta X$ in the analysis and defining a linear conductivity variation, $k_0 + \beta T$, across the melt interface. However, this proved unsuitable. The solution to the conduction equation given here is the only solution that handles properly the moving interface between the low-conductivity boundary layer and the high-conductivity liquid pool between the boundary layers.

III. COMPUTER CODE ORGANIZATION

EXPLO is written in FORTRAN IV. The main program is only a controller; as many input, output, and execution steps as possible are organized into subroutines. Data transmission between the subroutines is through four common blocks. The first contains the major arrays, such as temperature, which are used by most of the subroutines. The second contains layer-independent variables such as geometry definition and boundary conditions. The third contains layer-dependent variables such as dimensions, kinetics constants, and material properties. The fourth contains parameters that are generated by the code such as total heat, flux, and internal energy. A list of the inputs and their functions is in the Appendix.

Special features of some inputs and their effect on program execution need further discussion. The code calculates an average temperature for each time step, which, in turn, is used to calculate temperature-dependent material properties. Temperatures from a previous time step are stored in the T array, and new calculations are stored in the TT, or T' array. At the beginning of

each new time step, the T and TT arrays contain the same temperatures. If the number of variable property iterations (IKOUNT) is set to zero, the material properties are determined from the previous time step. However, if IKOUNT is set to one, the code first uses the previous temperatures to determine material properties and calculates the TT array. Then, the code determines material properties from the average of the T and TT arrays and calculates a new TT array. This process continues IKOUNT times. Normally, IKOUNT need not be set greater than one. However, for problems involving melt with internal convection, problems that burn beyond initiation (IDR or IDM = 2), or if the code output contains energy warning errors, IKOUNT may have to be set to three or greater.

Some problems involve a fixed flux at one boundary and a time-dependent temperature at the other boundary. Often the system should be allowed to equilibrate to a temperature distribution defined by the flux and the initial boundary temperature. If the ISS input is set to 1 (Card 2, see the Appendix), the code calculates an initial temperature distribution before it runs the transient analysis.

The code has a variable time step feature. If the maximum temperature change for all nodes is >4°C, the time step is decreased by half. If the maximum temperature change for all nodes is <10% of the maximum change allowable, the time step is increased by a factor of 2. If the initial time step is set to 0 or is not input, the code will calculate the initial time step.

The third card contains an input called GLOAD. GLOAD is a gravity-loading coefficient; it is used only by the internal convection routine to calculate the Grashof number. It is intended for use on studies involving the aerodynamic heating of an explosive beyond its melting point in aircraft or missile systems subject to aerodynamic forces other than gravity.

A point should be made about the code's operation in reacting boundary layer calculations. If a liquid explosive is heated through a boundary layer, thermal initiation occurs within the boundary layer. The code applies Nth-order kinetics to each element. In a real case, part of the explosive reacts, vaporizes, and floats away leaving a void to be filled. To represent this within the code, only for cases with internal convection (IDM = 2), the array that contains the burned fraction is reinitialized to zero before each calculation. Thus, each time step generates only the total energy available in an element, but that energy is replaced for the next time step. This use of the code gives better

results for the initiation of liquids; however, it invalidates the code's use for liquid burn problems.

If the energy initialization option is used, the code requires input of the average initial energy deposit (ENGA) and the front face energy deposit (ENGF) for each layer of material. The code then fits an exponential curve of the form

$$E_i = (ENGF)e^{-C_1 X} \quad , \tag{27}$$

where C_1 is selected such that the average energy criteria are met, E_i is the nodal initial energy, and X is the spatial distance.

The specific heat and thermal conductivity are defined as functions of temperature. The user may define the value of specific heat and conductivity for up to five temperatures. If a phase transition (such as melting) exists, the user can input the phase transition energy at any or all of the five temperatures. The computer code will linearly interpolate the defined values to determine the value at any temperature during the transient.

The use of Nth-order kinetics hints that the code may be valid for burn calculations. The reaction indicator (IDR) can be set equal to two, to allow the code to continue calculating beyond the initiation point. The code assumes that the heat is generated in the solid or liquid phase and is available for conduction from the generation point. In a real case the high explosive vaporizes and releases heat as gas. Any heat that is not lost must be convected and conducted back into the solid. Therefore, the code calculates reaction rates that may be considerably different than reality.

The user can simulate test configurations with the code and plot thermocouple data on the space plots generated by the code. If this option is used, inputs for the number of thermocouples (NTH) and the number of data points per thermocouple (NDATA) must be specified on Card 2. The code uses the thermocouple data to interpolate data points linearly in time and then places these points on the space plots.

IV. MATERIAL LIBRARY

A material library has been constructed to be compatible with the EXPLO computer code. This library (MATLIB) greatly reduces the time required to

prepare an input file. A library search is initiated if the user defines the reaction indicator (IDR) to be a number greater than 99. A list of the materials that are available for use with EXPLO is printed on the output file during each execution of the computer code. The data format used in the material library is the same as that used for the normal EXPLO input.

V. EXAMPLE PROBLEMS

EXPLO assumes that the user will have the figures output on the color FR80 system at Los Alamos. To reduce the amount of data that appears on each figure, EXPLO makes extensive use of color coding according to layer. Therefore, although some of the figures in this document may look confusing to the reader, the normal color film output will be clear.

From the many thermal analyses performed at Los Alamos, three were selected for simulation with EXPLO. The first is an analysis of a 2.54-cm-diam PBX 9502 sphere that was tested in the Los Alamos unconfined critical temperature test chamber.[6] This example shows the type of problems the code was designed to solve. The second example shows how the code can be used to calculate the temperature distribution of a plutonium-beryllium sandwich subjected to pulsed heating. The third example shows how a user may add a FORTRAN subroutine that can add energy (as a function of time) between layers of a composite. This particular example is a theoretical model that describes a potential mechanism by which HE is ignited during a skid impact.

A. PBX 9502 Sphere

We first prepared an input deck (Fig. 3) that consisted of a title card (line 1), two cards of control information (lines 2 and 3), three cards

```
 1  2.54 cm diameter 9502 sphere
 2      2    4    1   10  200    1     0     3     0     0     3     0                .5
 3     .0001  40000.          .0     293.0          0.          0.          .50
 4      .0          0.       293.
 5   1800.          0.       543.
 6  46800.          0.       543.
 7     10102  1    0.001     293.        0.          0.          0.          00.    pbx-9502
 8     20102  1    0.624     293.        0.          0.          0.          00.    pbx-9502
 9     20102  1    0.624     293.        0.          0.          0.          60.    pbx-9502
10     10102  1    0.001     293.        0.          0.          0.          00.    pbx-9502
*
```

Fig. 3.
Input deck for PBX 9502 sphere.

describing the transient temperature on the external surface (lines 4, 5, and 6), and four lines describing the material properties and geometry (lines 7 through 10). In this case, the material properties for PBX 9502 were found from material 102 in the material library. The sphere was divided into four layers to facilitate comparison of the analysis with test results. The terminal output (Fig. 4) shows the maximum temperature for each layer at each time. This particular analysis shows that we would have a thermal ignition at the center of the sphere after 2395 seconds.

```
2.54 cm diameter 9502 sphere
    TIME        MAXIMUM TEMPERATURE FOR EACH LAYER
                  1       2       3       4
 0.000000   293.    293.    293.    293.
    0.051   293.    293.    293.    293.
      26.   293.    293.    296.    296.
      92.   296.    297.    305.    305.
     157.   302.    305.    314.    314.
     223.   310.    313.    323.    323.
     289.   319.    322.    332.    332.
     354.   328.    331.    341.    341.
     419.   337.    340.    350.    350.
     485.   346.    349.    359.    359.
     551.   354.    358.    368.    369.
     616.   363.    367.    377.    378.
     682.   372.    376.    386.    387.
     747.   381.    385.    395.    396.
     813.   390.    394.    406.    405.
     878.   399.    403.    414.    414.
     944.   408.    412.    423.    423.
    1009.   417.    421.    432.    432.
    1075.   426.    430.    441.    441.
    1140.   435.    439.    450.    450.
    1206.   445.    448.    459.    460.
    1271.   454.    457.    468.    469.
    1337.   463.    466.    477.    478.
    1402.   472.    475.    486.    487.
    1468.   481.    485.    496.    496.
    1534.   490.    494.    505.    505.
    1599.   499.    503.    514.    514.
    1665.   508.    512.    523.    523.
    1730.   518.    521.    532.    532.
    1796.   527.    531.    541.    541.
    1861.   538.    540.    543.    543.
    1927.   545.    545.    545.    543.
    1992.   550.    550.    548.    543.
    2058.   553.    553.    550.    543.
    1000  SOLUTION ITERATIONS COMPLETED AT TIME =  0.800E+04
    2123.   556.    556.    558.    543.
    2189.   559.    559.    563.    543.
    2254.   562.    562.    564.    543.
    2320.   568.    566.    556.    543.
    2382.   580.    580.    560.    543.
 2394.931   615.    615.    562.    543.
 2395.392   642.    642.    562.    543.
 2395.437   667.    663.    562.    543.
 2395.440   703.    667.    562.    543.

IGNITION BEGINS AT DEPTH = 0.90E-03 CM IN LAYER  1
  2395.440 3026.    670.    562.    543.
PLOT    DONE.  PAGES =   25.  WORDS =    50374
GRAPHICS CL = U
$
```

Fig. 4.
Terminal output for PBX 9502 sphere.

The first frame on the film file contains a description of the geometry and a summary of the room-temperature material properties (Fig. 5). The subsequent plots that are printed on the film are dependent on the output option selected on card 2. For option 1, the code will generate a temperature versus space plot for the initial temperature distribution (Fig. 6) and the final temperature distribution (Fig. 7). If EXPLO had detected more than 0.1% decomposition of a high explosive (HE) component, it will also generate a burned fraction versus space plot (Fig. 8). EXPLO then generates plots of the boundary flux and internal heat generation versus time (Fig. 9) and temperature (Fig. 10), which are helpful when comparing EXPLO results with differential thermal analysis results. EXPLO then generates temperature versus time plots for each layer (Fig. 11) followed by a composite (Fig. 12) of all layers (the film output is color coded). Finally, EXPLO will generate plots of specific heat, internal energy, and conductivity versus temperature for each layer.

B. Plutonium-Beryllium Sandwich

This example demonstrates EXPLO's ability to deposit energy as a function of both space and time. The first three cards of the input deck (Fig. 13) are similar to those discussed in the first example. Lines 4 through 29 define a time-dependent multiplication factor (QFI - fourth column) for the internal heat generation. The geometry section (lines 30 through 41) is similar to the first example except for the energy generation term (QI) in the right-hand column of

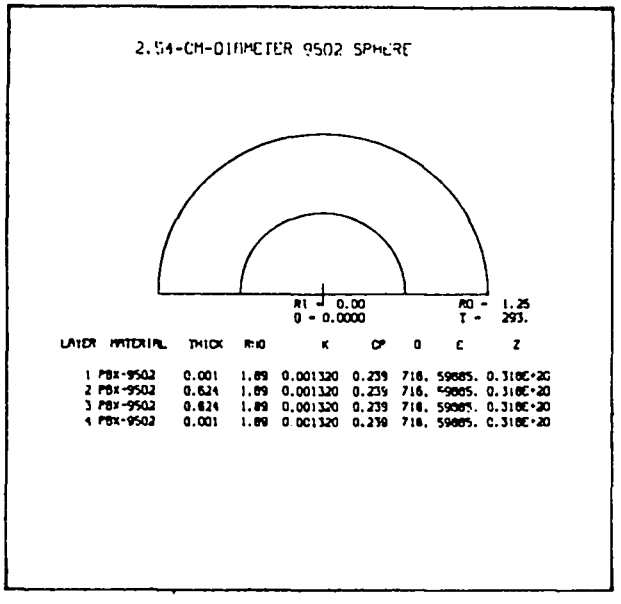

Fig. 5.
Geometry description and summary of room-temperature material properties (PBX 9502 sphere).

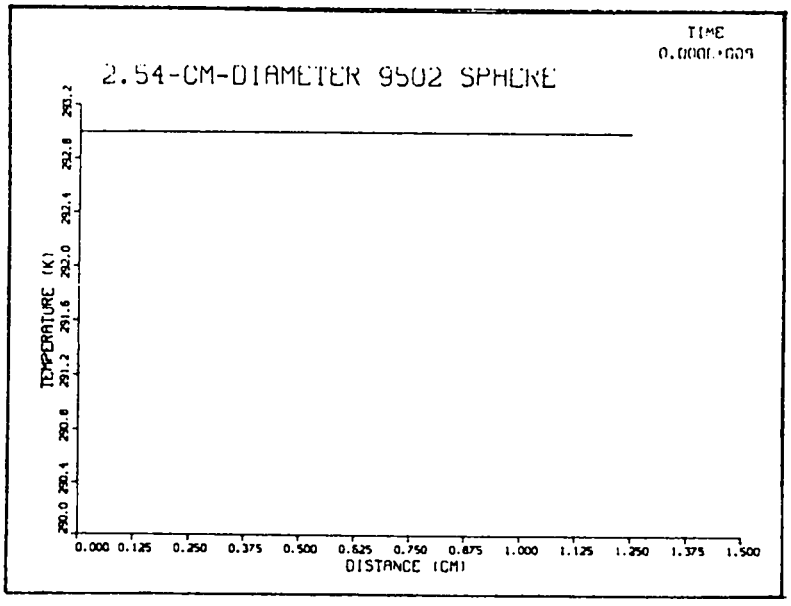

Fig. 6.
Temperature distribution for PBX 9502 sphere.

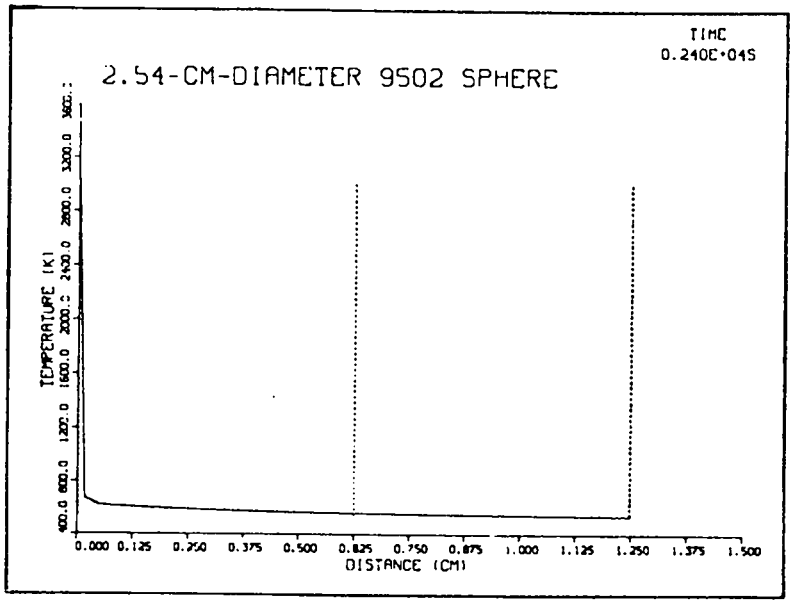

Fig. 7.
Final temperature distribution (PBX 9502 sphere).

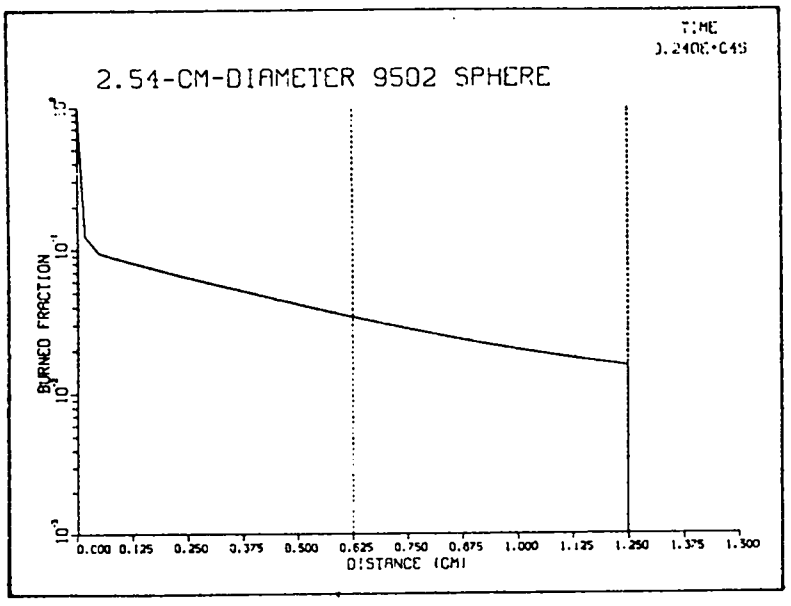

Fig. 8.
Burned fraction versus space plot (PBX 9502 sphere).

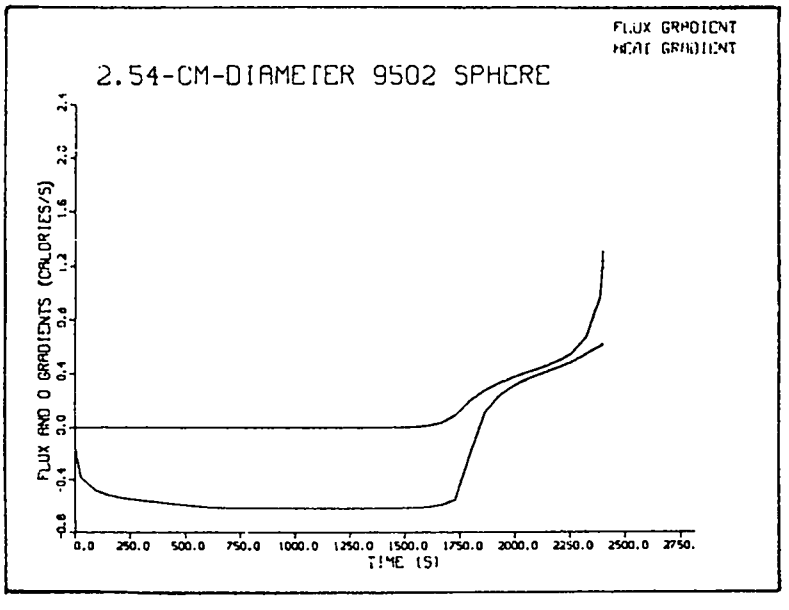

Fig. 9.
Boundary flux and internal heat generation versus time (PBX 9502 sphere).

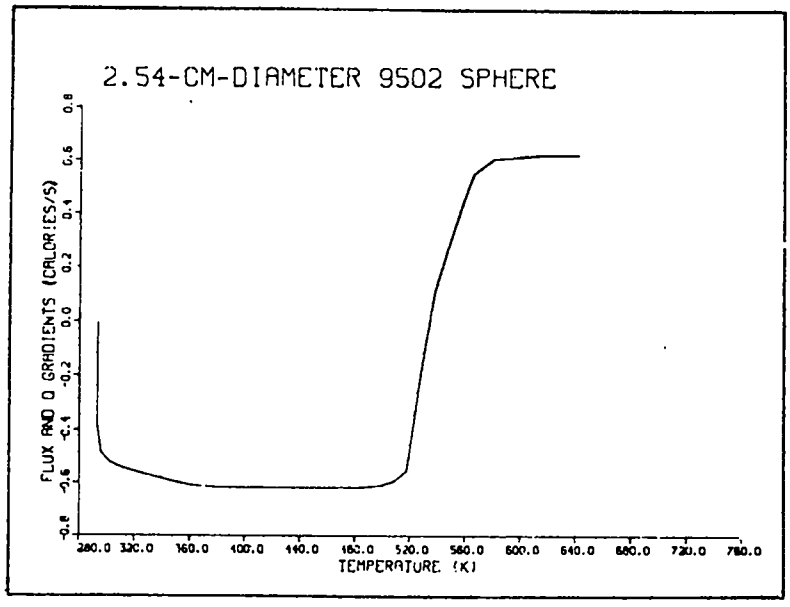

Fig. 10.
Boundary flux and internal heat generation versus temperature (PBX 9502 sphere).

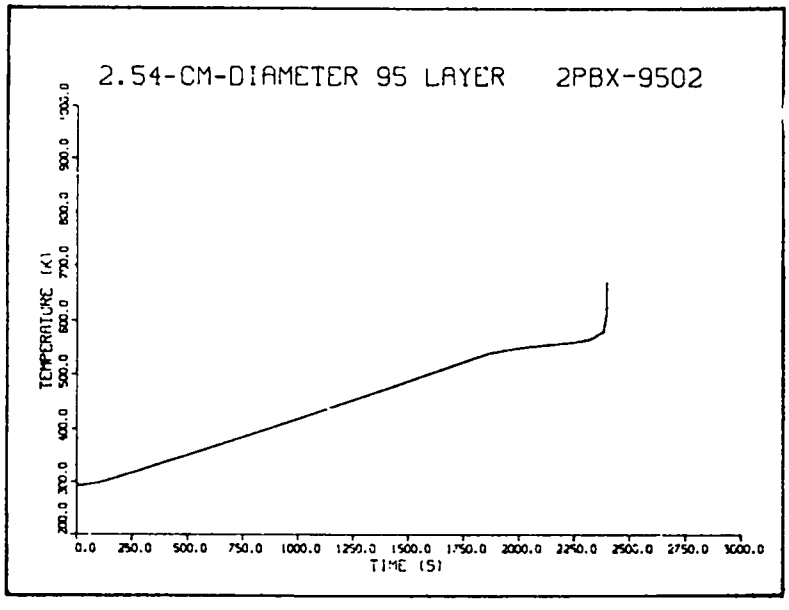

Fig. 11.
Temperature versus time (PBX 9502 sphere) (individual layer).

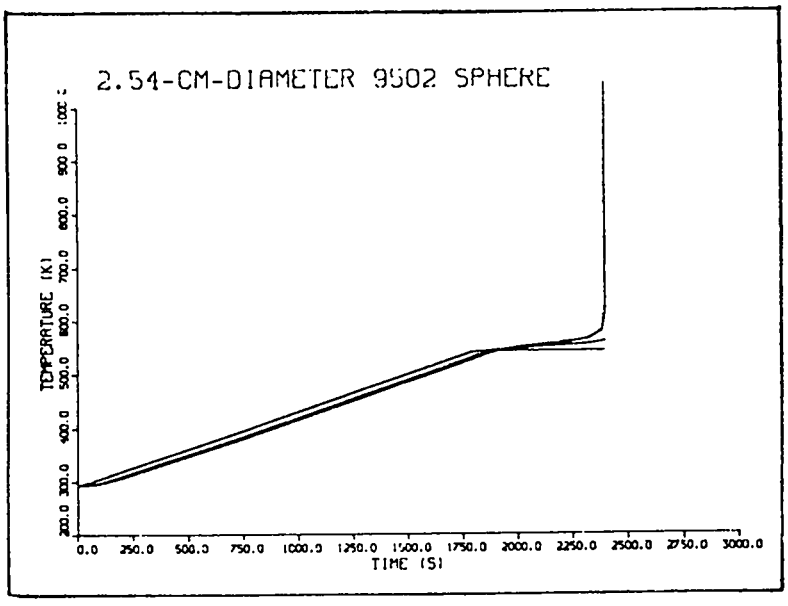

Fig. 12.
Temperature versus time (PBX 9502 sphere) (composite of all layers).

```
PU-BE SLAB STUDY
    0   12     1   10  199     1     1   26     0     0     3
  .0002              2.              0.
     0.            000.            000.            .021
  .0800            000.            000.            .263
  .0900            000.            000.            .672
  .1000            000.            000.           1.712
  .1100            000.            000.           4.120
  .1200            000.            000.           8.862
  .1300            000.            000.          15.043
  .1400            000.            000.          17.921
  .1500            000.            000.          14.469
  .1600            000.            000.           8.691
  .1700            000.            000.           4.815
  .1800            000.            000.           2.815
  .1900            000.            000.           1.816
  .2000            000.            000.           1.395
  .2100            000.            000.           1.151
  .2300            000.            000.           1.022
  .2500            000.            000.            .938
  .2900            000.            000.            .803
  .3300            000.            000.            .604
  .3700            000.            000.            .369
  .4100            000.            000.            .197
  .4500            000.            000.            .103
  .5000            000.            000.            .061
  .5500            000.            000.            .044
  .6000            000.            000.            .000
100.0000           000.            000.            .000
 5305   0          0.02            293.                                6.5
 5305   0          0.02            293.                                6.5
 5305   0          0.02            293.                                6.5
 5305   0          0.02            293.                                6.5
 5305   0          0.02            293.                                6.5
 5305   0          0.02            293.                                6.5
 5305   0          0.02            293.                                6.6
 5305   0          0.02            293.                                6.6
 5305   0          0.02            293.                                6.7
 5305   0          0.02            293.                                6.8
 5303   0           .290           293.                               00.0
 5303   0            .01           293.                               00.0
```

Fig. 13.
Input deck (plutonium-beryllium sandwich).

data. The magnitude of the internal heat generation for each time step is the product of QFI and QI. Therefore, the magnitude of either QFI or QI may be arbitrary but the other must be selected appropriately. The terminal output (Fig. 14) shows the maximum temperature for each layer as a function of time.

The first plot on the film file (Fig. 15) shows the geometry and provides a room-temperature summary of the material properties. EXPLO then generates several plots as described in the previous example, which include transient temperature plots for each layer (Fig. 16) and a composite transient temperature plot (Fig. 17). As previously described, EXPLO will follow these plots with material property plots for each layer.

```
PU-BE SLAB STUDY
    TIME        MAXIMUM TEMPERATURE FOR EACH LAYER
                  1      2      3      4      5      6      7      8      9     10     11     12
 0.000000      293.   293.   293.   293.   293.   293.   293.   293.   293.   293.   293.   293.
    0.077      295.   295.   295.   295.   295.   295.   295.   294.   294.   294.   293.   293.
    0.128      328.   328.   328.   328.   328.   328.   328.   327.   325.   317.   297.   293.
 0.136400      361.   361.   361.   361.   361.   361.   360.   358.   353.   337.   301.   297.
 0.146400      389.   389.   388.   388.   388.   388.   386.   382.   372.   350.   305.   294.
 0.154400      411.   411.   411.   411.   410.   409.   406.   400.   386.   358.   308.   295.
 0.162400      426.   426.   426.   426.   425.   423.   418.   409.   392.   361.   311.   295.
 0.170400      436.   436.   435.   435.   433.   430.   424.   412.   393.   360.   313.   297.
 0.178400      442.   442.   441.   440.   438.   434.   426.   413.   391.   359.   315.   298.
 0.186400      445.   445.   445.   443.   440.   434.   425.   411.   388.   357.   316.   299.
 0.194400      448.   448.   447.   444.   441.   434.   424.   408.   386.   355.   317.   301.
     0.204     450.   449.   448.   445.   441.   433.   422.   405.   383.   353.   318.   302.
     0.220     452.   451.   449.   445.   439.   431.   418.   401.   378.   351.   319.   305.
     0.236     452.   452.   449.   445.   438.   428.   415.   398.   376.   350.   320.   308.
     0.260     452.   451.   448.   443.   435.   425.   412.   395.   374.   350.   322.   311.
     0.292     450.   449.   446.   440.   432.   421.   408.   392.   372.   350.   325.   315.
     0.324     447.   446.   442.   437.   429.   418.   405.   389.   371.   350.   327.   318.
     0.356     443.   442.   438.   432.   425.   414.   402.   387.   370.   350.   329.   321.
     0.388     438.   437.   433.   428.   420.   410.   398.   384.   368.   350.   331.   324.
     0.420     432.   431.   428.   422.   415.   406.   394.   381.   366.   350.   333.   326.
     0.452     426.   425.   422.   417.   410.   401.   391.   378.   365.   350.   335.   329.
     0.484     420.   419.   416.   412.   405.   397.   387.   376.   363.   350.   336.   331.
     0.516     415.   414.   411.   407.   400.   393.   384.   373.   362.   350.   337.   332.
     0.548     409.   409.   406.   402.   396.   389.   381.   371.   361.   350.   338.   334.
     0.580     405.   404.   401.   398.   392.   386.   378.   369.   360.   350.   339.   335.
     0.612     400.   399.   397.   393.   389.   383.   376.   368.   359.   350.   340.   337.
     0.644     396.   395.   393.   390.   385.   379.   373.   366.   358.   350.   341.   338.
     0.676     392.   391.   389.   386.   382.   377.   371.   364.   357.   349.   342.   339.
     0.708     388.   387.   386.   383.   379.   375.   369.   363.   356.   349.   343.   340.
     0.740     385.   384.   382.   380.   377.   372.   367.   362.   356.   349.   343.   341.
     0.772     382.   381.   380.   377.   374.   370.   366.   361.   355.   349.   344.   341.
     0.804     379.   378.   377.   375.   372.   368.   364.   360.   355.   349.   344.   342.
     0.842     376.   375.   374.   372.   370.   366.   363.   359.   354.   349.   345.   343.
     0.906     371.   371.   370.   368.   366.   364.   360.   357.   353.   349.   345.   344.
     1000  SOLUTION ITERATIONS COMPLETED AT TIME =  0.913E+00
     0.970     368.   367.   367.   365.   363.   361.   359.   356.   353.   349.   346.   345.
     1.034     365.   364.   364.   363.   361.   359.   357.   355.   352.   349.   348.   345.
     1.118     361.   361.   361.   360.   359.   357.   355.   353.   351.   348.   347.   346.
     1.246     358.   358.   357.   357.   356.   355.   353.   352.   350.   349.   347.   347.
     1.412     354.   354.   354.   354.   353.   352.   352.   351.   350.   348.   348.   348.
     1.745     351.   351.   351.   351.   351.   350.   350.   350.   349.   349.   349.   348.
     2.154     351.   351.   351.   351.   351.   350.   350.   350.   349.   349.   349.   349.
PLOT    DONE.  PAGES =   56.  WORDS =   109084
GRAPHICS CL = U
$
```

Fig. 14.
Terminal output (plutonium-beryllium sandwich).

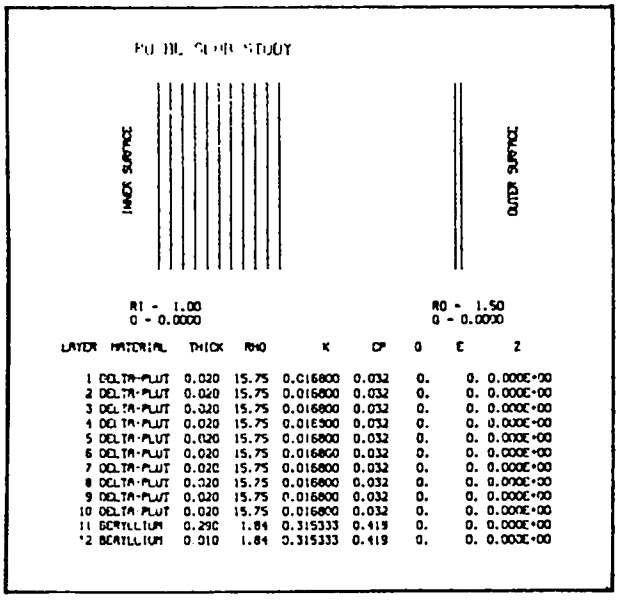

LAYER	MATERIAL	THICK	RHO	K	CP	Q	E	Z
1	DELTA-PLUT	0.020	15.75	0.016800	0.032	0.	0.	0.000E+00
2	DELTA-PLUT	0.020	15.75	0.016800	0.032	0.	0.	0.000E+00
3	DELTA-PLUT	0.020	15.75	0.016800	0.032	0.	0.	0.000E+00
4	DELTA-PLUT	0.020	15.75	0.016800	0.032	0.	0.	0.000E+00
5	DELTA-PLUT	0.020	15.75	0.016800	0.032	0.	0.	0.000E+00
6	DELTA-PLUT	0.020	15.75	0.016800	0.032	0.	0.	0.000E+00
7	DELTA-PLUT	0.020	15.75	0.016800	0.032	0.	0.	0.000E+00
8	DELTA-PLUT	0.020	15.75	0.016800	0.032	0.	0.	0.000E+00
9	DELTA-PLUT	0.020	15.75	0.016800	0.032	0.	0.	0.000E+00
10	DELTA-PLUT	0.020	15.75	0.016800	0.032	0.	0.	0.000E+00
11	BERYLLIUM	0.290	1.84	0.315333	0.419	0.	0.	0.000E+00
*2	BERYLLIUM	0.010	1.84	0.315333	0.419	0.	0.	0.000E+00

Fig. 15.
Geometry description and room-temperature summary of material properties (Pu-Be sandwich).

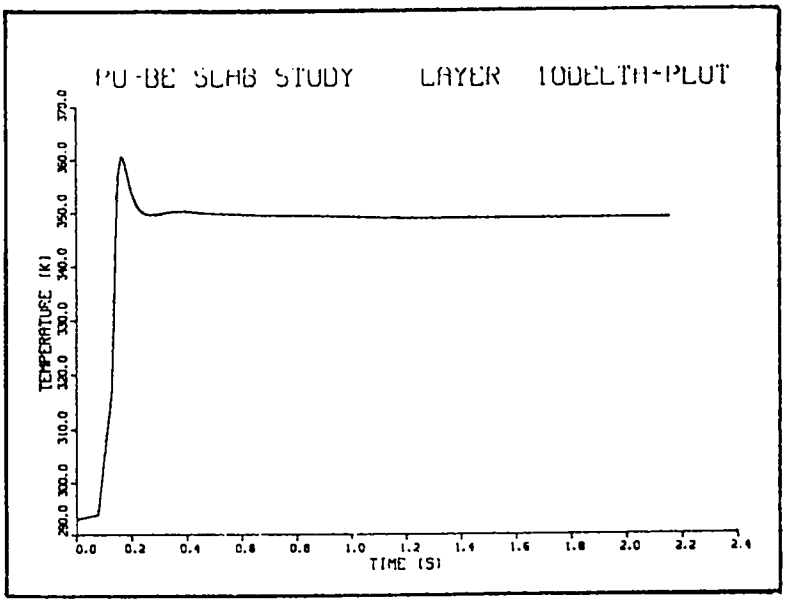

Fig. 16.
Transient temperature plot for individual layer (Pu-Be sandwich).

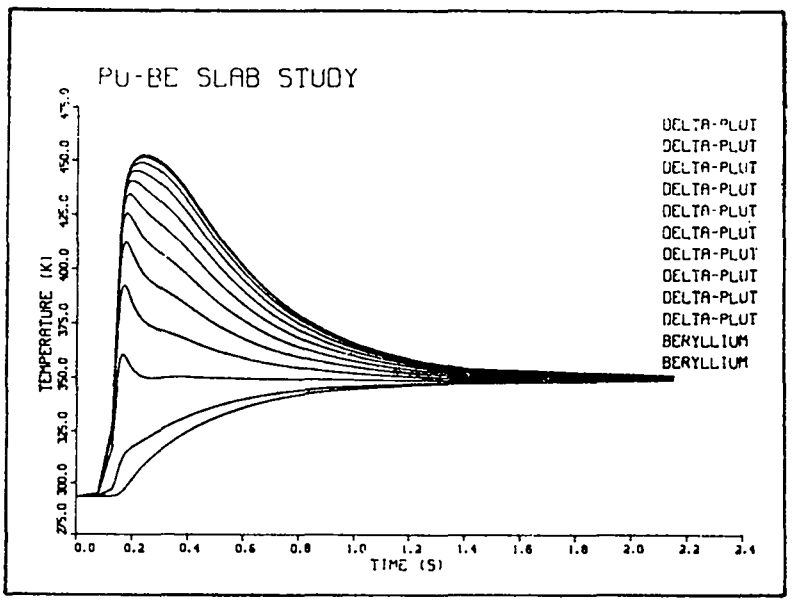

Fig. 17.
Composite transient temperature plot (Pu-Be sandwich).

C. Skid Model

EXPLO has also been modified, on several occasions, to accept user-defined routines that calculate energy input as a function of other variables. As an example, we developed one subroutine that calculated the energy generated by a sliding surface as a function of several variables and time. We are using this subroutine, with EXPLO, to try to understand better the initiation of HE caused by a skid impact. The subroutine requires one additional line of input data (line 9, Fig. 18) in the input file. The first input (the number 3) indicates the layer to the left of which the energy will be added. The second input is the drop height (cm), and the third is the weight (g). The fourth and fifth inputs are temperatures that correspond to shear strengths, the sixth and seventh inputs. The last input is the skid angle.

The first frame on the film output (Fig. 19) shows the geometry used for the calculation. We simulated the moving HE with a thick and a thin layer. We used the thin layer to obtain accurate calculations at the skid interface. The target was a gold layer, backed by a copper layer, which, in turn, was backed by an aluminum layer. The energy from skid was input between layers 2 and 3. The TTY output (Fig. 20) shows that the specimen rebounded 2.1 ms after impact. It also shows that, even though the HE was heated to 648 K, the specimen did

```
1  slab skid model 9501-gold
2      0     5     1  020  200     1     1     0     0     0     3     1                .5
3  .0000025    10.              .0          000.0          0.          0.          .50
4   30100  1     0.020   293.                  0.          0.          0.          00.     pbx 9501
5   50100  1     0.001   293.                  0.          0.          0.          00.     pbx 9501
6   25307  0      .6075  293.                  0.          0.          0.          00.     gold
7   25310  0      .0175  293.                  0.          0.          0.          00.     copper
8   25301  0      .2000  293.                  0.          0.          0.          00.     alum
9      3  500.     8670.          293.              554.              2.e09       2.6e08    45.
```

Fig. 18.
Input deck (skid model).

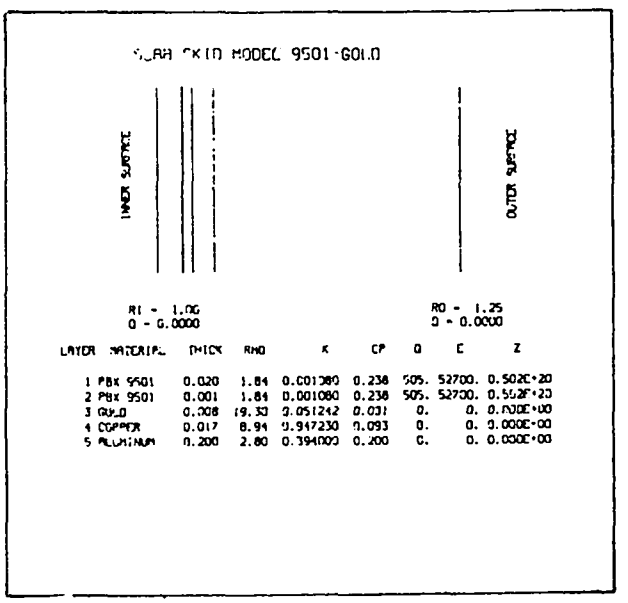

Fig. 19.
Geometry used for skid model calculation.

not ignite. The temperature distribution after rebound (Fig. 21) shows that this target was able to conduct heat away from the HE and thus prevent ignition. The burned fraction plot (Fig. 22) shows that 3% of the explosive at the interface has reacted. The flux gradient plot (Fig. 23) shows that the energy input was very high for approximately the first 10 μs while the HE was still cold and strong. By 25 μs, the HE has thermally softened at the interface, and the heat input is constant until rebound. The temperature of the HE at the interface increases rapidly for approximately 10 μs (Fig. 24). After 10 μs the HE is able to transfer most of the generated heat to the gold layer. The HE temperature does, however, continue to increase, but at a much lower rate. The

```
slab skid model 9501-gold
    TIME        MAXIMUM TEMPERATURE FOR EACH LAYER
                  1       2       3       4       5
0.000000        293.    293.    293.    293.    293.
0.000010        293.    478.    479.    293.    293.
0.000020        293.    502.    504.    293.    293.
0.000030        293.    516.    517.    293.    293.
0.000040        293.    524.    526.    296.    293.
0.000050        294.    530.    532.    297.    293.
0.000060        295.    536.    536.    301.    293.
0.000070        296.    538.    540.    306.    293.
0.000080        297.    541.    543.    311.    293.
0.000090        298.    543.    545.    315.    293.
0.000100        300.    545.    546.    320.    293.
0.000110        301.    547.    548.    324.    294.
0.000120        303.    548.    549.    328.    294.
0.000138        306.    549.    550.    336.    296.
0.000158        310.    550.    551.    341.    297.
0.000178        314.    551.    552.    347.    299.
0.000198        317.    552.    552.    352.    301.
   1000  SOLUTION ITERATIONS COMPLETED AT TIME =  0.211E-03
0.000218        321.    552.    553.    357.    304.
0.000246        326.    553.    553.    364.    307.
0.000286        333.    554.    554.    378.    313.
0.000326        339.    555.    553.    379.    318.
0.000366        345.    555.    553.    386.    324.
0.000406        350.    556.    554.    392.    329.
0.000446        355.    558.    555.    397.    334.
0.000486        360.    559.    557.    403.    339.
0.000526        364.    561.    559.    408.    344.
0.000560        368.    563.    560.    413.    348.
0.000580        370.    564.    561.    415.    350.
0.000600        372.    564.    562.    417.    353.
0.000620        375.    565.    563.    420.    355.
0.000638        377.    566.    564.    422.    357.
0.000646        378.    568.    564.    423.    358.
0.000656        380.    567.    565.    424.    359.
0.000668        381.    567.    565.    425.    360.
   2000  SOLUTION ITERATIONS COMPLETED AT TIME =  0.668E-03
0.000676        383.    568.    565.    426.    361.
0.000686        385.    568.    566.    428.    362.
0.000696        387.    569.    566.    429.    363.
0.000706        389.    569.    567.    430.    364.
0.000716        391.    569.    567.    431.    365.
0.000726        393.    570.    568.    432.    366.
0.000736        395.    570.    568.    433.    367.
0.000746        398.    571.    569.    434.    368.
0.000756        401.    571.    569.    435.    369.
0.000766        404.    572.    569.    436.    370.
0.000776        407.    572.    570.    437.    371.
0.000786        411.    572.    570.    438.    372.
0.000796        415.    573.    571.    439.    373.
0.000806        420.    573.    571.    440.    374.
0.000816        426.    574.    572.    441.    375.
0.000828        431.    575.    573.    443.    376.
   3000  SOLUTION ITERATIONS COMPLETED AT TIME =  0.845E-03
0.000848        440.    576.    574.    445.    378.
0.000868        448.    578.    576.    447.    380.
0.000888        456.    580.    577.    449.    382.
0.000908        461.    581.    579.    451.    384.
0.000928        467.    583.    581.    453.    386.
0.000948        472.    584.    582.    455.    388.
0.000986        481.    587.    585.    459.    391.
0.001028        489.    590.    588.    463.    396.
0.001066        496.    593.    591.    467.    398.
0.001106        503.    596.    594.    471.    402.
0.001146        509.    599.    597.    475.    405.
0.001186        514.    602.    599.    479.    409.
0.001250        522.    606.    604.    485.    414.
0.001330        530.    611.    609.    493.    421.
0.001410        538.    616.    614.    500.    428.
0.001490        545.    621.    619.    507.    434.
0.001570        552.    626.    624.    514.    441.
   4000  SOLUTION ITERATIONS COMPLETED AT TIME =  0.160E-02
0.001604        588.    621.    620.    517.    443.
0.001614        606.    618.    616.    518.    444.
0.001624        611.    619.    617.    518.    445.
0.001641        615.    621.    619.    519.    446.
0.001661        618.    623.    621.    520.    448.
0.001681        620.    625.    623.    521.    449.
0.001701        622.    626.    625.    523.    451.
0.001721        624.    628.    626.    524.    452.
0.001741        625.    630.    628.    526.    454.
0.001761        627.    631.    629.    527.    455.
0.001798        630.    634.    632.    530.    457.
0.001838        633.    636.    635.    533.    460.
0.001878        636.    639.    637.    536.    463.
0.001918        639.    642.    640.    539.    466.
0.001958        642.    645.    643.    542.    468.
0.001998        645.    647.    645.    545.    471.
0.002012        619.    642.    640.    546.    472.
   5000  SOLUTION ITERATIONS COMPLETED AT TIME =  0.201E-02
0.002028        625.    639.    637.    547.    473.
0.002038        629.    639.    637.    547.    474.
0.002042        638.    640.    638.    548.    474.
0.002052        633.    641.    639.    548.    475.
0.002062        635.    642.    640.    549.    476.
0.002079        637.    643.    641.    549.    477.
0.002099        639.    645.    643.    550.    478.
0.002119        642.    646.    645.    552.    479.
0.002139        644.    648.    646.    553.    481.
TIME AT REBOUND =0.2146E-02
0.002153        642.    641.    633.    554.    481.
0.002163        636.    633.    624.    554.    482.
0.002173        629.    626.    618.    554.    483.
0.002183        622.    620.    613.    553.    483.
0.002193        616.    614.    607.    553.    484.
0.002203        610.    608.    602.    552.    484.
0.002213        605.    603.    598.    551.    485.
   6000  SOLUTION ITERATIONS COMPLETED AT TIME =  0.222E-02
0.002223        600.    599.    593.    550.    486.
0.002243        592.    591.    586.    547.    487.
0.002263        586.    584.    579.    545.    487.
0.002283        580.    579.    573.    543.    488.
0.002303        575.    574.    568.    541.    489.
0.002328        570.    569.    562.    538.    489.
0.002364        570.    569.    562.    538.    490.
PLOT    DONE.  PAGES =   29.  WORDS =    57424
GRAPHICS CL = U
$ PTEKT
```

Fig. 20.
TTY output (skid model).

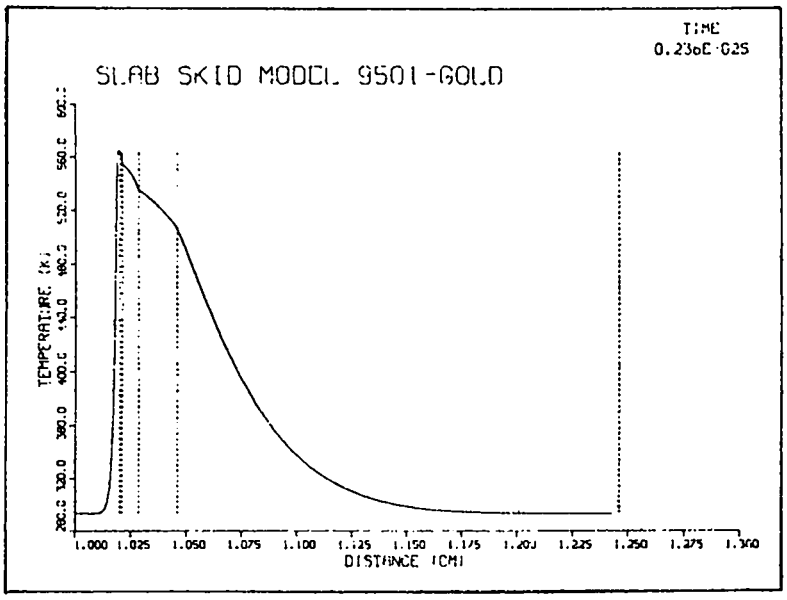

Fig. 21.
Temperature distribution after rebound (skid model)

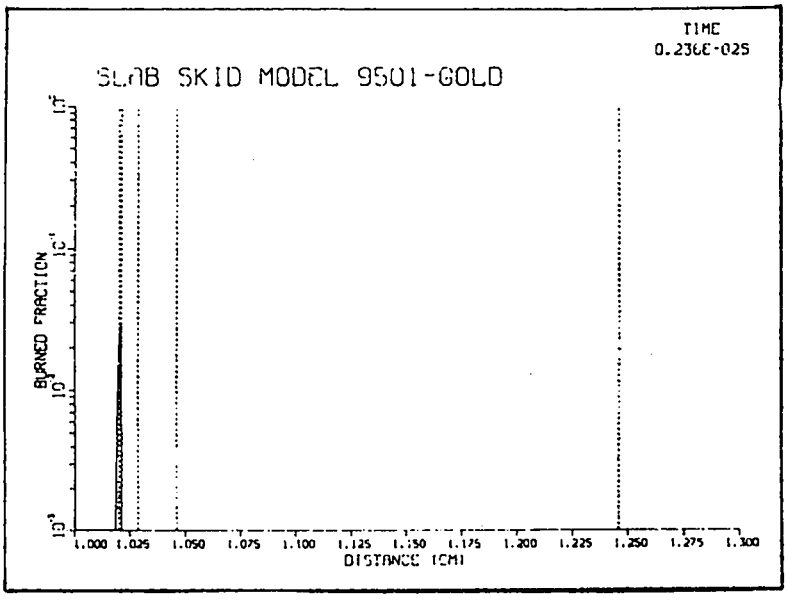

Fig. 22.
Burned fraction plot (skid model).

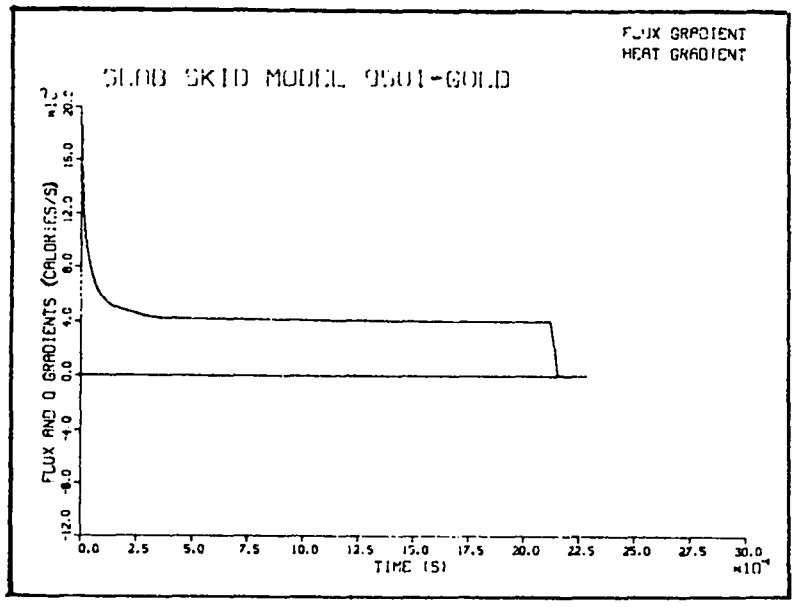

Fig. 23.
Flux gradient plot (skid model).

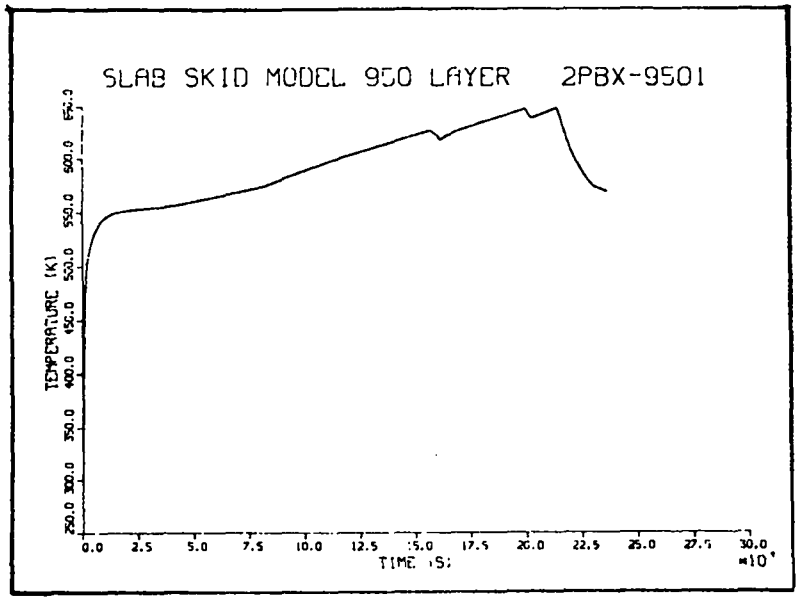

Fig. 24.
Transient temperature plot for individual layer (skid model).

temperature-time curve is not smooth, partly because of the phase transitions within the HE. The composite transient plot (Fig. 25) shows the complexity of the heat transfer that takes place. Finally, Figs. 26, 27, and 28 show the material property plots for PBX 9501.

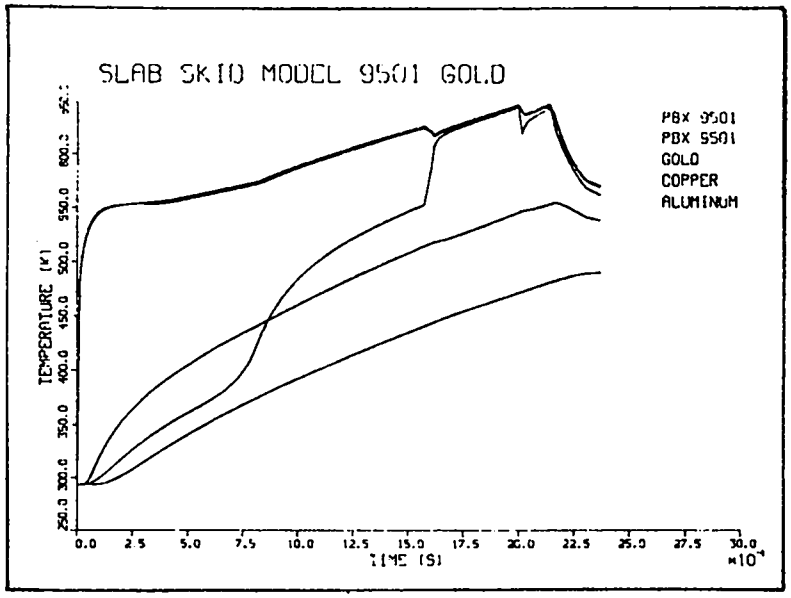

Fig. 25.
Composite transient temperature plot (skid model).

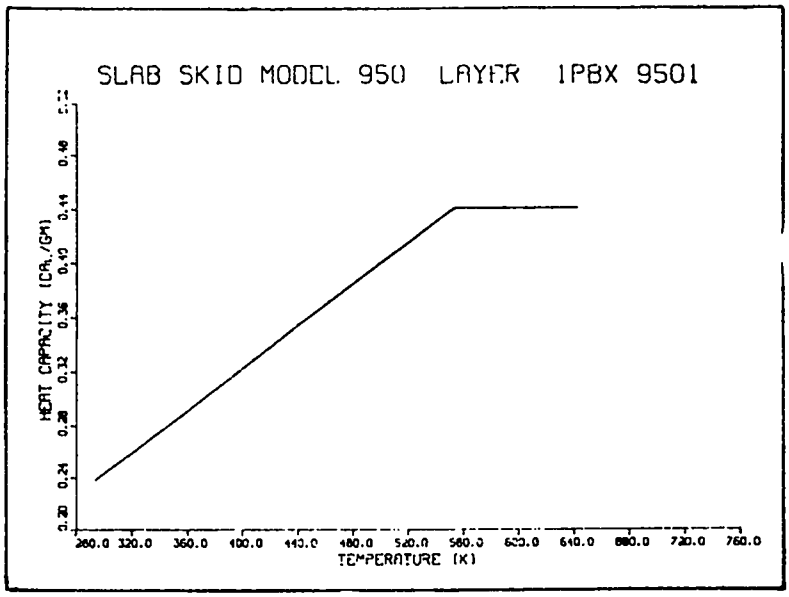

Fig. 26.
Heat capacity versus temperature (skid model)

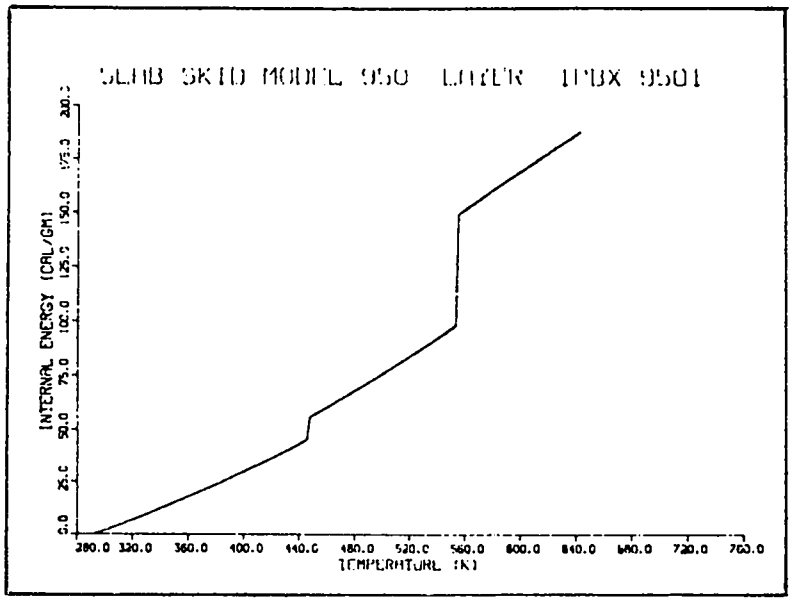

Fig. 27.
Internal energy versus temperature (skid model).

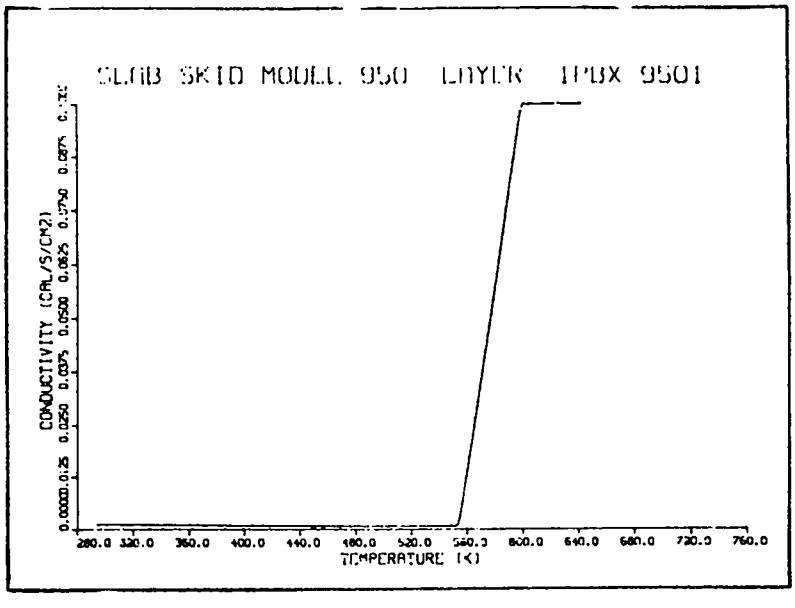

Fig. 28
Conductivity versus temperature (skid model).

REFERENCES

1. C. A. Anderson, "TEPLO: A Heat Conduction Code for Studying Thermal Explosions in Laminar Composites," Los Alamos Scientific Laboratory report LA-4511 (November 1970).

2. J. Zinn and R. N. Rogers, "Thermal Initiation of Explosives," J. Phys. Chem. 66, 2646 (1962).

3. A. J. Chapman, Heat Transfer, 3rd edition (MacMillan Publishing Co., Inc., New York, 1974).

4. A. Popolato, J. J. Ruminer, A. S. Vigil, N. K. Kernodle, and D. L. Jaeger, "Thermal Response of Explosives Subject to External Heating," Los Alamos Scientific Laboratory report LA-7667-MS (February 1979).

5. J. Crank and P. Nicholson, "A Practical Method for Numerical Evaluation of Solutions of Partial Differential Equations of the Heat-Conduction Type," Proc. Camb. Phil. Soc. 43, 50 (1947).

6. D. L. Jaeger, "Thermal Response of Spherical Explosive Charges Subjected to External Heating," Los Alamos Scientific Laboratory report LA-8332 (August 1980).

APPENDIX

EXPLO INPUTS

Card 1 5A10

1-60 - Title

Card 2 16I5

1- 5 - IGEOM - 0-Slab, 1-Cylindrical, 2-Spherical
6-10 - K - Number of layers (10 max)
11-15 - INDOUT - Output indicator
- 0-Time-temperature summary
- 1-Detailed time-temperature
- 2-Above plus plots
- 3-Above plus temperature of each node
16-20 - NCYC - Cycles per print
21-25 - NCYP - Number of cycles printed
26-30 - IIBC - Inner B.C.
- 0-Temperature
- 1-Flux
- 2-Convection
- 3-Conv-radiation
31-35 - IOBC - Outer B.C.
- 0-Temperature
- 1-Flux
- 2-Convection
- 3-Conv-radiation
36-40 - NOTIM - Number of time-dependent boundary conditions
41-45 - IDT - Variable time? 0-Yes, 1-No
46-50 - IZZY - Initialization, 0-Temperature, 1-Energy
51-55 - IKOUNT - Variable property iterations
56-60 - ISKID - 0-Normal, 1-For skid tests, 2-For hot wire initiation
61-65 - NTH - Number of thermocouple locations
66-70 - NDATA - Number of data points
71-75 - ISS - Initial steady-state indicator
76-80 - BETA - 0-Euler forward, .5-Crank-Nicholson, 1-Euler backward

Card 3 8E10

1-10 - DT - Initial time increment(s)
11-20 - TIMEMX - Maximum calculation time
21-30 - RI - Inner radius (cm)
31-40 - TQIB - Temp or flux on inner boundary (K, or cal/cm^2/s)
41-50 - TQOB - Temp or flux on outer boundary (K, or cal/cm^2/s)
51-60 - SSFR - Solid state reaction function
61-70 - VOLR - Initial HE volume ratio (<1.0)
71-80 - PRESMX - Maximum container containment pressure (atmos)

Next Card (If External Convection or Radiation) 8E10.3

1-10 - DIM - Characteristic dimension (cm)
11-20 - ALT - Altitude - (meters)

21-30 - VELOC - Velocity (m/s)
31-40 - DELTAM - Ambient temperature deviation from standard
41-50 - EMIS - Emissivity
51-60 - TOR - Radiation temperature base

New Card(s) (If Time-Dependent Boundary) 8E10.3

1-10 - TIMB - Time(s)
11-20 - TQIB - Temperature or flux on inner boundary (K, cal/cm^2/s)
21-30 - TQOB - Temperature or flux on outer boundary (K, cal/cm^2/s)
31-40 - QFI - Time-dependent multiplication factor for QI
41-50 - QFJ - Time-dependent multiplication factor for QJ
51-60 - ALT - Time-dependent altitude, transient convection
61-70 - VELOC - Time-dependent velocity (m/s), transient convection
71-80 - QRAD - Radiation flux

Next Card(s) (1-Each Layer) I4, 2I3, 6F10.0, A10

1- 4 - NNL - Number of elements per layer
5- 7 - IDR - Reaction, 0-No, 1-Yes, 2-Continue analysis beyond initiation, if >99, find all material data in material library
8-10 - IDM - Melt, 0-no, 1-yes, 2-internal convection
11-20 - THICK - Thickness of layer (cm)
21-30 - TAVI - Initial average temperature (K)
31-40 - ENGA - Initial average energy (cal/gm^3)
41-50 - ENGF - Initial front face energy (cal/gm^3)
51-60 - QI - Internal heat generation (cal/g/s)
61-70 - QJ - Heat generation at interface (cal/cm^2/s)
71-80 - MTL - Material label

Next Card(s) (If IDM=2) 8E10.3

1-10 - VISC(1)- Viscosity coefficient
11-20 - VISC(2)- Viscosity coefficient
21-30 - VISC(3)- Viscosity coefficient
31-40 - BET - Coefficient of thermal expansion

Next Card(s) (5 maximum) 10F10.0

1-10 - TMLT - Transition temperature
11-20 - RHO - Density (g/cm^3)
21-30 - CP - Specific heat (liquid phase, cal/g/K)
31-40 - EK - Conductivity (liquid phase, cal/cm/s/K)
41-50 - HTFUS - Heat of fusion (cal/g)
51-60 - E - Activation energy (cal/mole)
61-70 - Q - Heat release (cal/g)
71-80 - Z - Frequency factor (1/s)
81-90 - ORDR - Reaction order
91-100- SPFR - Species fraction (can be 0 for last)

For Each Above Card (5 maximum) 10F10.0

51-60 - E - Activation energy (cal/mole)

61-70 - Q - Heat release (cal/g)
71-80 - Z - Frequency factor (1/s)
81-90 - ORDR - Reaction order
91-100- SPFR - Species fraction (can be 0 for last)
End with a blank card

Next Card(s) (If Test Data) 20E6.0 (There should be NTH points)

1-100- RTST - Location of each thermocouple

Next Card(s) (If Test Data) 20E6.0 (There should be NDATA cards)

1-10 - TIMTST - Time of thermocouple reading
11-100- TEMTST - Thermocouple temperatures

NOMENCLATURE

Symbol	Description
C	Constant
$CC = \frac{\Delta r^2}{\alpha \Delta \tau}$	Coefficient of finite difference equation
$C_1 = 1 - \frac{k\Delta r}{2r}$	Geometry coefficient
$C_2 = 1 + \frac{k\Delta r}{2r}$	Geometry coefficient
D_{ij}	Matrix coefficient
E_j	Activation energy of jth component
h	Convection coefficient
K	Thermal conduction coefficient
i,j,k,l,m,n,	Exponent or subscript
N	Number of explosive species present
N_{GR}	Grashof number
N_{NU}	Nusselt number
N_{PR}	Prandtl number
N_{RE}	Reynolds number
Q_j	Energy of decomposition
QI	Internal energy generation
QJ	Interface energy generation
R	Gas content
S_j	Initial species concentration
T	Temperature
T_{AMB}	Ambient temperature
T_{BL}	Boundary layer temperature

Symbol	Description
T_w	Wall temperature
T_R	Ambient temperature for radiation
V	Force vector
W_j	Species present at any given time
ΔX	Incremental distance
ΔX_{eff}	Effective boundary layer thickness
Z	Collision number
α	Thermal diffusivity
ε	Emissivity
Δ, δ	Denotes difference
$\eta_i = \frac{K_i \Delta X_j}{K_j \Delta X_i}$	Coefficient in difference equation
ρ	Density
σ	Stefan-Boltzmann Constant
τ	Time

Printed in the United States of America
Available from
National Technical Information Service
US Department of Commerce
5285 Port Royal Road
Springfield, VA 22161

Microfiche $3.50 (A01)

Page Range	Domestic Price	NTIS Price Code	Page Range	Domestic Price	NTIS Price Code	Page Range	Domestic Price	NTIS Price Code	Page Range	Domestic Price	NTIS Price Code
001-025	$ 5.00	A02	151-175	$11.00	A08	301-325	$17.00	A14	451-475	$23.00	A20
026-050	6.00	A03	176-200	12.00	A09	326-350	18.00	A15	476-500	24.00	A21
051-075	7.00	A04	201-225	13.00	A10	351-375	19.00	A16	501-525	25.00	A22
076-100	8.00	A05	226-250	14.00	A11	376-400	20.00	A17	526-550	26.00	A23
101-125	9.00	A06	251-275	15.00	A12	401-425	21.00	A18	551-575	27.00	A24
126-150	10.00	A07	276-300	16.00	A13	426-450	22.00	A19	576-600	28.00	A25
									601-up	†	A99

†Add $1.00 for each additional 25-page increment or portion thereof from 601 pages up.